

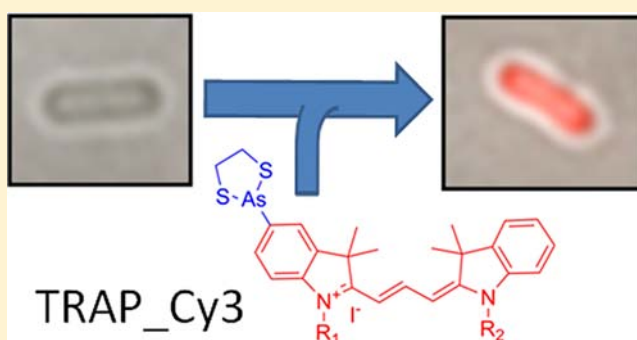
Synthesis and Application of an Environmentally Insensitive Cy3-Based Arsenical Fluorescent Probe To Identify Adaptive Microbial Responses Involving Proximal Dithiol Oxidation

Na Fu, Dian Su, John R. Cort, Baowei Chen, Yijia Xiong, Wei-Jun Qian, Allan E. Konopka, Diana J. Bigelow, and Thomas C. Squier*

Biological Sciences Division, Fundamental Sciences Directorate, Pacific Northwest National Laboratory, Richland, Washington 99352, United States

S Supporting Information

ABSTRACT: Reversible disulfide oxidation between proximal cysteines in proteins represents a common regulatory control mechanism to modulate flux through metabolic pathways in response to changing environmental conditions. To enable *in vivo* measurements of cellular redox changes linked to disulfide bond formation, we have synthesized a cell-permeable thiol-reactive affinity probe (TRAP) consisting of a monosubstituted cyanine dye derivatized with arsenic (i.e., TRAP_Cy3) to trap and visualize dithiols in cytosolic proteins. Alkylation of reactive thiols prior to displacement of the bound TRAP_Cy3 by ethanedithiol permits facile protein capture and mass spectrometric identification of proximal reduced dithiols to the exclusion of individual cysteines. Applying TRAP_Cy3 to evaluate cellular responses to increases in oxygen and light levels in the photosynthetic microbe *Synechococcus* sp. PCC7002, we observe large decreases in the abundance of reduced dithiols in cellular proteins, which suggest redox-dependent mechanisms involving the oxidation of proximal disulfides. Under these same growth conditions that result in the oxidation of proximal thiols, there is a reduction in the abundance of post-translational oxidative protein modifications involving methionine sulfoxide and nitrotyrosine. These results suggest that the redox status of proximal cysteines responds to environmental conditions, acting to regulate metabolic flux and minimize the formation of reactive oxygen species to decrease oxidative protein damage.



INTRODUCTION

The reversible oxidation of proximal cysteines to form cystine commonly modulates enzyme function, and their site-specific oxidation may represent a means to differentially shift cellular metabolism in response to a range of environmental inputs to adjust metabolic flux so as to maintain optimal cellular function and minimize the widespread irreversible oxidative damage to a range of proteins that can lead to cell death.¹ For example, in oxygenic phototrophs changes in light intensity or oxygen concentrations are associated with the production of reactive oxygen species (ROS),² which can directly oxidize cysteines and other amino acids.^{1f} Complicating a mechanistic understanding of relationships between cysteine post-translational modifications (PTMs) and cellular function are the multiple functional roles of cysteines in biology. Cysteines may act as nucleophiles in active sites, chelation sites for metal binding, carriers of nitric oxide, and sites of disulfide bond formation.^{1e,3} Further, while multiple chemical probes have been developed that target redox-active (hyper-reactive) cysteines that commonly involve a reactive thiolate intermediate, it is currently not possible to differentiate between cysteines involved in intramolecular disulfide bond formation from

individual reactive thiols associated with other pathways involving redox signaling (e.g., S-glutathionylation or S-nitrosylation).⁴ Thus, while changes in the oxidation state of redox-active sulfhydryl groups are broadly understood to modify cellular signaling and metabolic flux in response to changes in cellular redox conditions as well as ROS formation,⁵ a precise understanding of the cellular significance of specific PTMs requires an ability to distinguish, for example, highly reactive active site cysteines from cysteines far from the active site that form mixed disulfides (e.g., cystines) as part of a redox-dependent regulatory mechanism. An important technical problem involves an ability to identify PTMs to cysteines that authentically occur intracellularly, as cell lysis can result in the air oxidation of cysteines and the formation of mixed disulfides unrelated to those found under physiological conditions. The ability to trap and visualize proximal reduced cysteines in cellular proteins prior to cell lysis is invaluable when coupled with mass spectrometric approaches that subsequently identify these modifications.

Received: December 4, 2012

Published: February 4, 2013

Cell-permeable cysteine reactive probes have been reported that monitor variations in cysteine reactivity in cellular environments, with applicability for affinity isolation and proteomic identification to determine hyper-reactive sites that may have regulatory importance.⁶ In the case of sulfenic acid intermediates, live cell trapping and imaging measurements involve the selective reaction of dimedone to form a stable conjugate suitable for affinity isolation and mass spectrometric identification.⁷ Likewise, the applicability of arsenicals for the affinity purification of proteins with vicinal thiols has been extended to permit *in situ* imaging using the cell permeable monoarsenical fluorescent probe NPE based on the chromophore naphthalimide.⁸ However, the fluorescence intensity of naphthalimides are sensitive to the local molecular environment, exhibiting “a low quantum yield in aqueous solution, but becoming highly fluorescent in nonpolar solvents or when bound to hydrophobic sites in proteins or membranes”.⁹ As reactive sites for NPE in eukaryotic cells have been suggested to largely involve proteins in membranes (i.e., mitochondria and endoplasmic reticulum), and to be low in the cytoplasm and nucleus—their suboptimal fluorescence properties prevent quantitative conclusions.^{8a} Furthermore, subsequent mass spectrometric based approaches that identify proximal disulfides following affinity capture have not previously been developed, which has limited a molecular understanding of how redox-dependent control mechanisms regulate metabolism.

To permit quantitative measurements of changes in the cellular redox state of proximal cysteines, we have synthesized a thiol-reactive affinity probe (TRAP) based on the photostable and environmentally insensitive cyanine chromophore derivatized with an arsenic atom capped with ethanedithiol (EDT) (i.e., TRAP_Cy3). Alkylation of unreactive thiols prior to displacement of the bound TRAP_Cy3 by ethanedithiol permits facile protein capture and mass spectrometric identification of labeling sites.¹⁰ TRAP_Cy3 is demonstrated to monitor changes in disulfide bond status in response to growth conditions using microbes in culture and using natural microbial mat samples collected at Yellowstone National Park.¹¹ An inverse relationship is observed between disulfide bond formation and the abundance of methionine sulfoxide [Met(O)] and nitrotyrosine (NY) in cellular proteins, suggesting an important role for disulfide bond formation in limiting the formation of ROS-dependent PTMs.

■ EXPERIMENTAL PROCEDURES

Microbial Cultivation. Unless specified, *Synechococcus* sp. PCC7002 cells were grown in chemostats, essentially as previously described,¹² at 30 °C in the presence of 40 mM NaHCO₃ (pH 7.5), 17 mM NH₄Cl, 8 mM KCl, 2 mM CaCl₂, 40 mM MgSO₄, 0.55 mM H₃BO₃, 0.20 μM MnCl₂, 2 μM ZnCl₂, 0.05 μM CoCl₂, 0.2 μM Na₂MoO₄, 0.00001 mM CuSO₄, and 0.1 mM EDTA.

Immunoblotting. Proteins were electrophoretically separated by SDS-PAGE using duplicate 4–12% gradient gels, with MES running buffer (Invitrogen, Carlsbad, CA); one gel was stained with Coomassie blue protein stain; the other, used for immunoblotting. Immunoblotting involved transfer of separated proteins to a PVDF membrane (2 h, 30 V) prior to blocking with 5% nonfat milk in 50 mM Tris-HCl (pH 7.6), 150 mM NaCl, and 0.05% Tween20 for 1 h. Commercially available primary polyclonal antibodies were used to detect Met(O) (1:1,000) (Cayman Chemicals, Milwaukee, WI) and NY (1:1,000) (Bioscience Resource Project, Saco, ME). A dilution of 1:1000 of secondary antibody conjugated with horseradish peroxidase (immunoPur Antibody, Pierce, Rockford, IL) was used for chemiluminescence detection with

SuperSignal West Femto maximum Sensitivity Substrate (Pierce), using a Lumi-Imager for gel imaging.

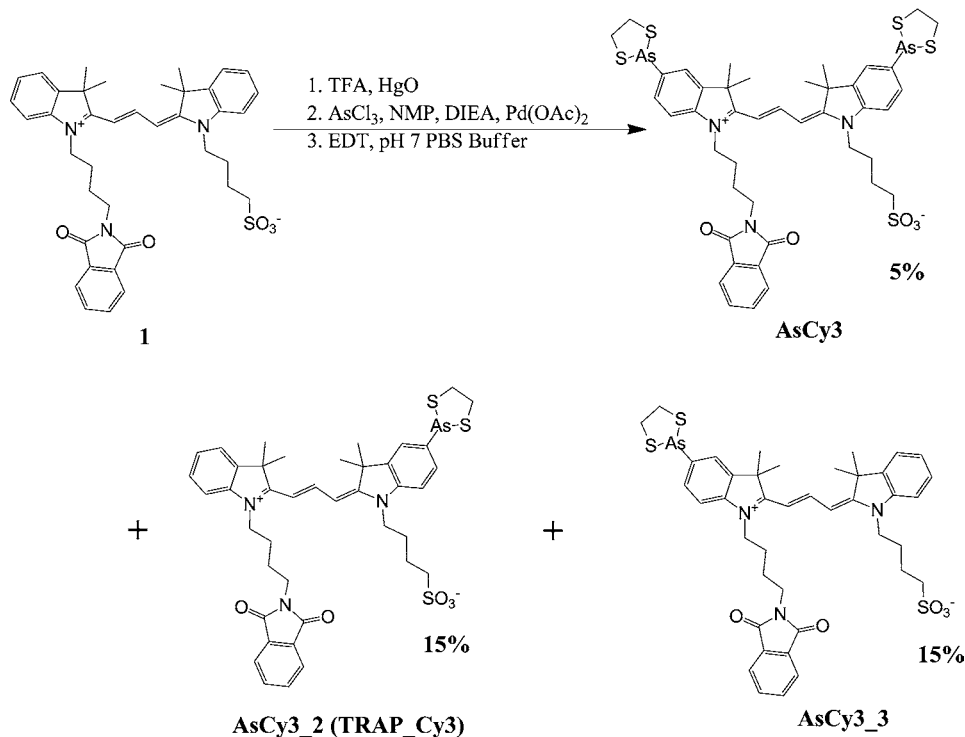
Live-Cell Labeling by TRAP_Cy3. *Synechococcus* sp. PCC7002 cells (OD_{730nm} ≈ 0.5) were incubated with 0.5 μM TRAP_Cy3 in growth media for 30 min at room temperature. In order to remove unbound TRAP_Cy3, cells were washed (pelleted) seven times prior to lysis in 25 mM HEPES (pH 7.7), where washing steps 2 and 3 included 5 mM β-mercaptoethanol, and washing steps 4 and 5 included 2.5% (w/v) bovine serum albumin (BSA). Cells were lysed using a French press with 2 × 10⁴ psi four times. Lysates were pelleted at 2.4 × 10⁴ g at 4 °C for 20 min, and supernatants were collected. A standard BCA assay (Pierce) was used to measure protein concentrations.

In Vitro Protein Labeling by TRAP_Cy3. Individual purified proteins [thioredoxin (Trx), BSA, and calmodulin (CaM)] (1 mg/mL) in 25 mM HEPES (pH 7.6), 150 mM NaCl, and 200 μM tris(2-carboxyethyl)phosphine (TCEP) were incubated overnight at 4 °C to reduce cysteines prior to incubation with TRAP_Cy3 or compound 1 (100 μM, unless otherwise indicated) for 1 h at room temperature with shaking (800 rpm). Proteins were separated from unreacted probe by centrifugal filtration [3 kDa (Trx and CaM) or 10 kDa (BSA) molecular mass cutoff].

Selective Enrichment of TRAP_Cy3-Bound Proteins/Peptides. Mixed disulfides in TRAP_Cy3-labeled/unlabeled BSA (0.1 mg/mL) were reduced with 1 mM TCEP in 25 mM HEPES (pH 7.7) for 1 h at 37 °C with constant shaking (800 rpm) prior to alkylation with 10 mM *N*-ethylmaleimide and 10 mM iodoacetamide (0.5 h at 37 °C with constant shaking at 500 rpm in the dark). After reaction, samples were repeatedly washed (4×) to remove the excess alkylation reagents in 8 M urea using Amicon Ultra-4 centrifugal filters (10 kDa molecular weight cutoff) (EMD Millipore, Billerica, MA). Total volumes were adjusted to 150 μL prior to the addition of 1 mM EDT to displace bound TRAP_Cy3. Solutions were incubated for 45 min at 600 rpm to ensure release of the TRAP_Cy3 probe from the labeled protein prior to loading onto a Hande Mini-Spin column containing 35 mg of prewet and prewashed thiopropyl Sepharose 6B resin with water and 25 mM HEPES (pH 7.7) and incubated at room temperature for 2 h with shaking (850 rpm) to affinity capture reduced thiols, as previously described.¹³ Nonspecifically bound proteins were washed from the resin using 0.5 mL × 5 times each of (unless specified) (i) 8 M urea, (ii) 2 N NaCl, (iii) 80% acetonitrile/0.1% trifluoroacetic acid (TFA), and (iv) 25 mM HEPES buffer (pH 7.7). For LC-MS/MS detection, bound proteins were subjected to trypsin digestion (50 μg/mL) in 25 mM HEPES (pH 7.7), 0.1% SDS, and 1 mM CaCl₂ at 60 °C for 3.5 h with constant shaking (850 rpm), and unbound peptides were extensively washed from the resin (see above). Finally, bound peptides were released from the resin upon incubation with 20 mM DTT (30 min) prior to incubation with 80% acetonitrile/0.1% TFA (10 min) at room temperature (850 rpm). In each step, eluted cysteinyl peptides were collected as flow-through by centrifuging the spin column at 1500g for 1 min, and were concentrated in a speed vac and reconstituted to a final volume of 30 μL in water for subsequent analysis.

LC-MS/MS Detection. Enriched cysteine-peptide samples were analyzed using a fully automated, custom-built, four-column capillary liquid chromatography (LC) system coupled online to an LTQ-Orbitrap mass spectrometer (Thermo Fisher Scientific, San Jose, CA) via an electrospray ionization (ESI) interface manufactured in-house.¹⁴ The 75 μm (inner diameter) × 65 cm fused silica capillary reversed-phase column (Polymicro Technologies, Phoenix, AZ) was prepared using the slurry packing procedure with 3 μm diameter Jupiter C18 bonded particles (Phenomenex, Torrance, CA) at 8000 psi. Peptides were loaded and separated using an exponential gradient starting with 100% mobile phase solvent A (0.1% formic acid in water), and gradually increased to 60% solvent B (0.1% formic acid in 100% acetonitrile) over 100 min with a flow-rate of ~500 nL/min over the separation column. The instrument was operated in data-dependent mode with an *m/z* range of 400–2000 with a resolution of 100K for full MS scans. The six most abundant ions from the MS analysis were selected for MS/MS fragmentation using a normalized collision energy

Scheme 1. Synthesis of Monoarsenic Probe TRAP_Cy3



setting of 35% with a dynamic exclusion duration of 1 min. The heated capillary temperature was 200 °C, and the spray voltage was 2.2 kV.

RESULTS

Synthesis of a Monoarsenical Cyanine Fluorescent Probe (TRAP_Cy3). TRAP_Cy3 was prepared by mercuration and a subsequent transmetalation reaction with arsenic of an unsymmetrical Cy3 starting material (compound 1),¹⁵ where phthalimide and sulfonate functionalities are expected to enhance cellular delivery to permit binding to dithiols in cytosolic proteins (Scheme 1). The unsymmetrical Cy3 starting material (compound 1), was prepared as previously described with satisfying yield (80%).¹⁶ Following mercuration and transmetalation to arsenic, products were liganded to EDT for enhanced stability.¹⁷ The one pot reaction resulted in a mixture of products including a disubstituted AsCy3 (5%), a monoarsenic AsCy3_2 (15%), a monoarsenic AsCy3_3 (15%), as well as unreacted starting materials. Resulting compounds were separated using thin layer chromatography, and structures were identified using 2D NMR (see Supporting Information, Figure S1 and Table S1 for experimental procedures and chemical shift assignments). For AsCy3_2, the arsenic is specifically inserted para to the nitrogen of the indole ring with a sulfonate tail; the opposite arrangement between the inserted arsenic and indole ring is observed for AsCy3_3. There is an increased mobility (R_f) for AsCy3_2 ($R_f = 0.39$) in comparison to AsCy3_3 ($R_f = 0.37$) using 7% methanol in methylene dichloride. Differences in R_f values may arise due to the more amphiphilic features of AsCy3_3 in comparison to AsCy3_2 because of the positioning of the arsenic motif. Consistent with this interpretation, AsCy3_2 demonstrates substantially improved live cell labeling in comparison to AsCy3_3 (Figure S2), which is probably the result of enhanced cellular permeability, and represents the optimal sensor of reduced proximal dithiols in live cells. In comparison with Cy3

(compound 1; $\lambda_{\max} = 558$ nm), the fluorescence spectrum of TRAP_Cy3 is red-shifted by 10 nm ($\lambda_{\max} = 568$ nm); there are minimal differences in quantum yield (Figure S3). Accordingly, AsCy3_2 (i.e., TRAP_Cy3) was used for subsequent measurements to demonstrate the utility of this reagent.

Specific and High-Affinity Binding to Proximal Reduced Cysteines. To assess the specificity of TRAP_Cy3 to selectively recognize proximal reduced cysteines, we monitored binding for three proteins that differ in the number of cysteines and their propensity to form dithiol pairs. In the case of Trx there are two redox-active cysteines (i.e., Cys33 and Cys36 in Trx from *Escherichia coli*); high-affinity binding in the reduced state (following addition of 300 μ M TCEP) is apparent from significant changes in the steady-state polarization upon binding TRAP_Cy3 (Figure 1). No appreciable increase in polarization is observed between TRAP_Cy3 and oxidized Trx; likewise, as compound 1 (no arsenic) does not bind reduced Trx it is apparent that the probe itself neither selectively partitions into the binding cleft nor binds single cysteines. Rather, binding and stabilization of TRAP_Cy3 requires the presence of a pair of reduced cysteines. The high-affinity binding between TRAP_Cy3 and Trx ($K_d = 80 \pm 20$ nM) is comparable to prior reports that characterized the association between biarsenical cyanine probes complexed with EDT and tetracysteine binding sequences,^{17,18} suggesting that observed binding constants correspond to the initial association of one arsenic with a dithiol pair in the peptide tagging sequence.

To further clarify the requirement for proximal cysteines for TRAP_Cy3 binding, we compared the reactivities using an engineered protein (i.e., C4-CaM) with proximal introduced cysteines (i.e., EEQIAE¹¹ to CCQICC¹¹) previously used to demonstrate the binding specificity of biarsenical probes with a mutant CaM containing a single highly exposed reactive cysteine (i.e., Thr110Cys).^{7a,19} Following incubation of

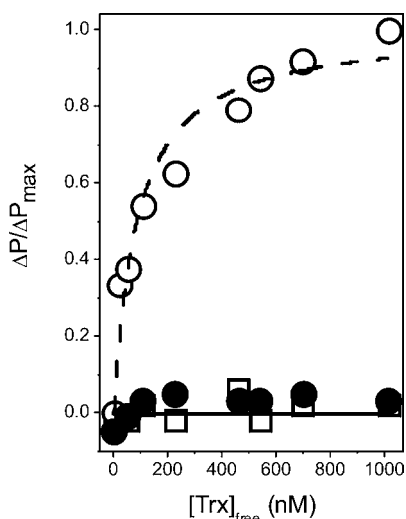


Figure 1. Increases in TRAP_Cy3 polarization upon binding thiothredoxin (Trx). Polarization of TRAP_Cy3 (circles) or compound **1** (open squares) (25 nM) following incubation with reduced Trx (open symbols) or oxidized Trx (filled circles). Dashed curve represents the nonlinear least-squares fit to a Langmuir binding curve ($K_d = 80 \pm 20$ nM). Unbound (free) concentrations of Trx were calculated as $[\text{Trx}]_{\text{free}} = [\text{Trx}]_{\text{total}} - \Delta P/\Delta P_{\text{max}}[\text{Trx}]_{\text{total}}$.

TRAP_Cy3 under reducing conditions (200 μM TCEP) and separation of unreacted probe from labeled proteins using SDS-PAGE, it is apparent that TRAP_Cy3 selectively binds vicinal cysteines; no detectable binding is apparent between TRAP_Cy3 and the single introduced cysteine in a mutant CaM (i.e., Thr110Cys) (Figure 2B).

Finally, to address possible interference from reactive unpaired cysteines and hydrophobic binding clefts, we assessed the binding of TRAP_Cy3 to BSA (UniProtKB P02769), which contains 17 proximal cysteine pairs that form disulfide bonds and one hyper-reactive cysteine (i.e., Cys₅₇) previously shown to be highly reactive and to be preferentially alkylated.²⁰ In the presence of reducing agent (0.2 mM TCEP), BSA was incubated with TRAP_Cy3 and compound **1** to assess binding specificity. Following separation by SDS-PAGE and visualization of the fluorescence signal, it is apparent that only TRAP_Cy3 selectively binds the reduced BSA (Figure 2A). There is no binding between TRAP_Cy3 and air-oxidized BSA (no added TCEP; data not shown), emphasizing that the binding complex was formed through the arsenic motif and proximal reduced cysteine pairs (as clarified below).

Affinity Capture and Mass-Spectrometric Identification of Dithiol Pairs. Validation of binding interactions and an understanding of regulatory mechanisms require an ability to identify redox-active cysteines that participate in disulfide bond formation through their affinity capture and mass-spectrometric identification. Using BSA to evaluate the utility of using TRAP_Cy3 to identify cysteines that form disulfide bonds, we assessed the ability to selectively bind and identify reduced cysteine pairs. All accessible protein vicinal dithiols in reduced BSA were labeled by TRAP_Cy3. Excess TRAP_Cy3 was removed by centrifugal filtration (10 kDa molecular mass cutoff). Available unreacted cysteines were alkylated using 10 mM iodoacetamide and 10 mM *N*-ethylmaleimide in the presence of 1 mM TCEP. After removal of excess alkylating agents, bound TRAP_Cy3 was subsequently displaced upon incubation with 1 mM EDT, and following TRAP_Cy3

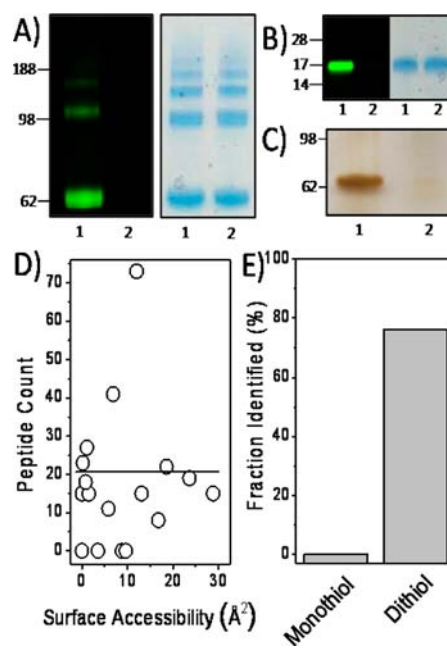


Figure 2. Selective targeting of TRAP_Cy3 to proximal reduced cysteines permits affinity purification and site identification. (A) Fluorescence image (left) and protein stain (right) following separation by SDS-PAGE for 20 μM bovine serum albumin (BSA) previously reduced with TCEP (0.2 mM) and incubated with 100 μM TRAP_Cy3 (lane 1) or compound **1** (lane 2) for 1 h; 0.2 μg of protein loaded onto each lane of gel. (B) Fluorescence image (left) and protein stain (right) following separation by SDS-PAGE for 60 μM calmodulin (CaM) incubated with 100 μM TRAP_Cy3, corresponding to mutants possessing proximal reduced cysteines (lane 1) or a single reduced cysteine (i.e., Thr110Cys in CaM) (lane 2); 0.1 μg of protein is loaded onto each lane of gel. (C) Silver stain images following separation on SDS-PAGE subsequent to affinity capture using thiopropyl Sepharose 6B resin for TRAP_Cy3 labeled BSA (lane 1) or unlabeled BSA (lane 2). Prior to affinity capture BSA was alkylated (10 mM iodoacetamide and 10 mM *N*-ethylmaleimide) and treated with EDT (1 mM) to release bound TRAP_Cy3. (D) Sum of peptide count from mass spectrometry measurements for proximal cysteines that form disulfide bonds (PDB 1NSU) in comparison to calculated surface accessibility for sulfur atoms calculated using the program Surface Racer using a probe diameter of 1 \AA .³² In calculating the surface accessibility of individual sulfurs to the monoarsenic probe we used a radius of 1 \AA to reflect the smaller ionic radius of arsenic (ionic radius is 0.5–0.6 \AA), instead of the 1.4 \AA commonly used for water (1.4 \AA overall radius). Line represents the average peptide count for all peptides involved in disulfide bonding. (E) Fraction of identified peptides containing hyperreactive Cys57 (monothiol) or peptides that form disulfide bonds in oxidized albumin (dithiol).

displacement the available cysteines were used to affinity capture proteins using a thiol reactive resin. The resin was washed according to a previously reported method,²¹ and enriched protein was released by DTT (see Experimental Procedures). In comparison, BSA without bound TRAP_Cy3 was fully alkylated, and was not captured by the affinity resin (Figure 2C).

For mass spectrometric identification, immobilized BSA was subjected to trypsin digestion (60 $^{\circ}\text{C}$) and isolated peptides were subjected to LC-MS/MS identification. Thirteen of the 17 pairs of cysteines (i.e., dithiols) were identified (i.e., 76%); in comparison, hyper-reactive Cys57 (monothiol) was never observed (Figures 2E and S4, and Table S2). Further, only

4% of identified peptides did not contain a cysteine, consistent with the binding specificity of TRAP_Cy3 for proximal cysteines. Similar peptide counts (a measure of abundance) were obtained irrespective of the calculated surface accessibilities of the paired sulfur atoms in the crystal structure, which varied from near 0 to almost 30 Å² (Figure 2D). In comparison, the surface accessibility of the sulfur in Cys57 is 26 Å², which is substantially larger than the surface accessibility of any other individual sulfur atom in the other 34 cysteines in BSA. These results indicate that binding of TRAP_Cy3 permits the selective identification of reactive dithiol pairs.

Live-Cell Imaging. Critical to the utility of TRAP_Cy3 as an *in vivo* probe of the physiologically relevant redox status of proximal cysteines is an ability to rapidly partition into the cytosol in living cells. To test cell permeability, we expressed a tagged engineered protein with proximal introduced cysteines (i.e., C4-CaM) in *E. coli*. The vast majority of cells are labeled, as in apparent in overlays between the bright-field and fluorescence imaging (Figure 3). Under these conditions no

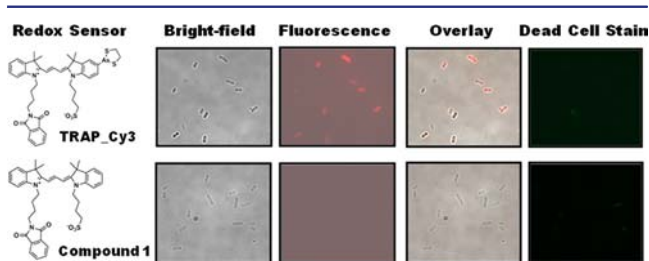


Figure 3. Live-cell labeling by TRAP_Cy3. Images of *E. coli* following incubation with TRAP_Cy3 (top) or compound 1 (bottom) (0.5 μM), showing entire cellular population (bright-field), fluorescence, and overlay relative to imaging any dead cells with SYTOX green nucleic acid stain (5 μM) (<http://products.invitrogen.com/ivgn/product/S7020>), which is cell impermeable and undergoes a 500-fold fluorescence enhancement upon binding to nucleic acids. $\lambda_{\text{ex}} = 530$ nm and $\lambda_{\text{em}} = 570$ nm (TRAP_Cy3); or $\lambda_{\text{ex}} = 488$ nm and $\lambda_{\text{em}} = 520$ nm (SYTOX@Green).

dead cells are detected using SYTOX Green (from Life Technologies Corp.). In comparison, the control (compound 1 with no arsenic) is not retained in living cells, ensuring that fluorescence signals can be interpreted in terms of the abundance of reduced cysteines. These results demonstrate the cell-permeability of TRAP_Cy3 and the ability to visualize redox-active proximal cysteines in living bacterial cells.

Shifts in Redox Status of Proximal Cysteines following Environmental Perturbations. We investigated the capability of TRAP_Cy3 to react with redox-active dithiols in the cyanobacterium, *Synechococcus* sp. PCC7002 under different environmental conditions that could be experienced by cyanobacteria in nature. These included low and high values for dissolved oxygen tension (DOT, i.e., 1% and 50%) and for light intensity (i.e., 650 and 1720 μmol m⁻² s⁻¹).²² These measurements involved chemostat cultures grown at steady-state. As endogenous chromophores, such as phycocyanin (PC) and other antennae pigments, interfere with the selective detection of the fluorescence of TRAP_Cy3 in living cells, redox-dependent changes in disulfide bond formation were monitored following cell lysis and protein separation by SDS-PAGE (Figure 4A). Large differences in the intensity of TRAP_Cy3 staining were observed under these different environmental conditions, indicating substantial changes in

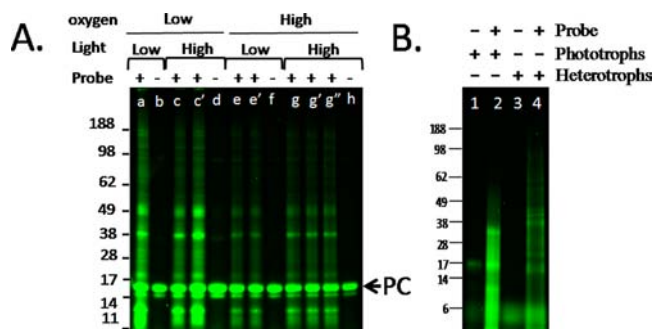


Figure 4. Environmentally induced changes in the redox status of proximal cysteines. TRAP_Cy3 fluorescence intensity following SDS-PAGE separation of cellular lysates obtained from *Synechococcus* sp. PCC7002 grown in bioreactors (A) and field samples of microbial mats from Yellow Stone National Park (B). Prior to cell lysis, phototrophic and heterotrophic cells within the microbial mat layers were physically separated. Cells grown in bioreactors were cultivated in the presence of low (600 μmol m⁻² s⁻¹) or high (1700 μmol m⁻² s⁻¹) light levels; dissolved oxygen tension (DOT) was either low (1%) or high (50%). Other growth conditions are as described in Experimental Procedures. Samples a, c, e, and g were incubated with TRAP_Cy3 immediately upon collection from the bioreactor. Samples c' and g' were stored in the dark for 2 h before treatment. Samples e' and g'' were bubbled with argon for 30 min, either under room light or in the dark prior to incubation with TRAP_Cy3. The abundant endogenous pigment phycocyanin (PC) in *Synechococcus* sp. PCC7002 migrates near 16 kDa (panel A). In all cases, live-cell labeling involved incubation with TRAP_Cy3 (5 μM) for 30 min prior to cell lysis and visualization of fluorescence ($\lambda_{\text{ex}} = 530$ nm and $\lambda_{\text{em}} = 570$ nm).

the status of redox-active proximal cysteines. Irrespective of growth conditions or incubation with TRAP_Cy3 the abundance of the antennae protein PC remains essentially unchanged, as indicated by the similar intensities of the bright band that migrates with an apparent mass near 16 kDa following protein separation by SDS-PAGE. Thus, alterations in disulfide bond formation are consistent with a model involving functional regulation, and are unlikely to be the result of differences in captured photons and the metabolic formation of reducing equivalents (e.g., NADPH) that directly modify overall cellular redox levels.

Comparisons of TRAP_Cy3 staining in *Synechococcus* 7002, grown under conditions where the DOT was maintained at a very low level (1% DOT), indicate substantial reductions in the abundance of redox-active proximal cysteines at high light intensities (1700 μmol m⁻² s⁻¹) in comparison to cells grown at lower (but still photosynthetically saturating) light intensities (600 μmol m⁻² s⁻¹), which are largely reversed following incubation in the dark for two hours (Figure 4A). Although one might hypothesize that regulation at the level of gene expression would decrease the number and size of photosynthetic units to minimize damage at high light intensities, the results suggest that PTMs involving disulfide bond formation between proximal cysteines play a significant regulatory role even under these steady-state growth conditions. At higher DOT (50%), but still well below what is present in natural environments, there are dramatic reductions in bound TRAP_Cy3 relative to what was observed at high light intensities but low DOT; these decreases in the abundance of reduced proximal cysteines in response to increases in DOT were found at both low and high light intensity. This indicates that redox control mechanism may act to shift metabolic fluxes when DOTs are higher, in which case proximal cysteines are

oxidized to form cystines irrespective of light levels. Further, in contrast to samples grown at low DOT, there was minimal recovery in the abundance of reduced proximal cysteines after dark incubation or following reduction of DOT. These latter results suggest a reduction in reductant pools at high oxygen concentrations, which limit the ability for a rapid recovery of metabolic potential.

In comparison to the relatively oxidized state of proximal cysteines in cells grown in the presence of high oxygen (and nonlimiting carbon and nitrogen sources) (Figure 4A, lane e), there are significant increases in the abundance of reduced proximal cysteines for *Synechococcus* 7002 grown under carbon-limited (but not nitrogen-limited) conditions (Figure S5). These observations are consistent with a hypothesis that carbon limitation reduces flux through the Calvin cycle, acting to favor a more reducing cellular environment. The nitrogen-limited cultures provide a useful comparison as other physiological characteristics (growth rate) were identical. These results suggest that the status of redox-active proximal cysteines in cellular proteins may signal the intracellular physiological state and help regulate metabolic flux.

The utility of TRAP_Cy3 to monitor redox potentials of proximal cysteines in natural environments was assessed following incubation of natural microbial mats in hot springs from Yellowstone National Park, which form layered communities with photosynthetic autotrophic microbes in an upper layer (1 mm thick) and heterotrophic microbes lower in the mat (about 3 cm thick).²³ Upon incubation of TRAP_Cy3 with intact microbial mats prior to the separation of the phototrophs and heterotrophic microbial layers, it is apparent that in comparison to the heterotrophs that there are substantially larger numbers of cellular proteins that contain redox-active proximal cysteines in the photosynthetic microbes (Figure 4B). These results are consistent with the known role of redox-active disulfide switches in the control of photosynthetic proteins in the thylakoids of higher plants,^{3c,24} and is consistent with a similar regulatory role in cyanobacteria where hyper-reactive cysteines are concentrated in the thylakoid membrane (see Figure S6).

Oxidative Damage to Cellular Proteins. Light-induced formation of ROS has the potential to oxidatively damage a range of cyanobacterial proteins; a major function of cellular reductant (e.g., glutathione, Trx, and NADPH) is to detoxify ROS, and to reduce oxidatively damaged amino acid side chains, including cysteines, methionines, and tyrosines²⁵ (Figure S7). We have used antibodies against Met(O) and NY to assess possible abundance changes in these oxidatively modified amino acids in *Synechococcus* 7002 grown at potentially damaging light intensities and oxygen concentrations. Representative immunoblots are shown (Figure 5) from lysates of cells (i.e., *Synechococcus* sp. 7002) grown in chemostats under highly reproducible controlled conditions. At both high light and high oxygen levels, there is a 70% decrease in total Met(O) and a 40% decrease in total NY formation in comparison to cells grown at both low light and low oxygen levels (Figure 5). Low to intermediate levels of protein oxidation are observed at either high light or high oxygen. Three major protein targets of methionine oxidation, with apparent molecular masses of 16, 54, and 67 kDa, represent 90% of total Met(O) staining (Figure 5A). Substantial reductions in staining against Met(O) (albeit to differing levels) are apparent for all three bands under high light or high oxygen conditions (Figure 5A). Likewise, there are reductions

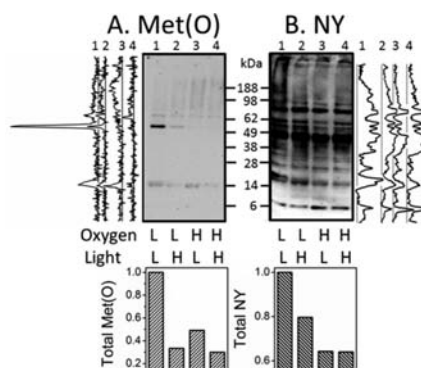


Figure 5. Global reductions in protein oxidative damage at high light and oxygen. Immunoblot detection of Met(O) (A) or nitrotyrosine (NY) (B) following separation on SDS-PAGE of lysates from *Synechococcus* sp. PCC7002 grown in chemostats at variable light or oxygen levels. Densitometric scans showing individual band intensities are alongside immunoblots. Bottom panels show total integrated intensities of each lane in immunoblots. Low (L) or high (H) oxygen respectively correspond to 1% and 50% DOT. Low (L) or high (H) light levels respectively correspond to 600 and 1700 $\mu\text{mol m}^{-2} \text{s}^{-1}$. Protein loads were 20 μg per lane. Positions of molecular mass standards are indicated.

in the abundance of NY staining for the majority of proteins when cells are grown under conditions of high light, high oxygen, or both (Figure 5B). Thus, under conditions associated with dramatic increases in the oxidation of proximal cysteines, as detected by TRAP_Cy3 (see Figure 4), there are no corresponding increases in global protein oxidation as detected by Met(O) and NY; in fact, there are modest decreases. Such an inverse relationship between the oxidation of proximal cysteines and other sensitive amino acids (i.e., Met and Tyr) is consistent with a mechanism involving the formation of cystine that modifies enzymatic function to alter metabolic flux, acting to decrease rates of ROS formation and the widespread oxidation of methionines and tyrosines in cellular proteins (a common indication of oxidative stress) to enhance photo-tolerance in *Synechococcus* sp. 7002.

DISCUSSION

We have synthesized a cell-permeable, monoarsenic probe (TRAP_Cy3) that selectively binds to proximal dithiols, permitting the trapping and visualization of redox-active cysteines in living cells (Figures 3 and 4). Following cell lysis, TRAP_Cy3-bound proteins can be visualized using SDS-PAGE and, following displacement of TRAP_Cy3 by EDT, proteins can be affinity isolated for mass spectrometric identification of the cysteine labeling sites (Figure 2 and Table S2). The utility of TRAP_Cy3 as a capture reagent for cysteines relies on several important characteristics, including (i) optimal hydrophobicity that permits facile cellular delivery; (ii) inclusion of arsenic that enables selective and high-affinity binding to proximal reduced cysteines (i.e., $K_d = 80 \pm 20$ nM) (Figures 1 and 2); (iii) incorporation of the EDT cap that stabilizes the arsenic, thus reducing binding kinetics relative to diffusion rates for uniform sampling; and (iv) use of a cyanine scaffold that permits accurate measurements of changes in the redox status of proximal cysteines irrespective of local cellular environment (for example, upon partitioning into microcompartments, such as thylakoid membranes). TRAP_Cy3 thus offers the ability to monitor global changes in disulfide bond formation between

proximal cysteines, and insights into how redox-active cysteines control cellular metabolism, without artifacts common to approaches that require cell lysis prior to affinity isolation. In conjunction with measurements of protein oxidative modification in *Synechococcus* sp. PCC7002 grown under environmentally relevant conditions, TRAP_Cy3 has revealed a correlation between the increased oxidation of proximal cysteines and decreases in protein oxidative damage that may be part of a regulatory strategy to modify metabolic flux to minimize ROS formation and associated protein oxidative damage (Figures 5 and 6).

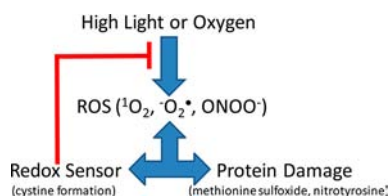


Figure 6. Proposed relationship between the oxidation of proximal cysteines in response to increases in ROS generation and the oxidative damage of other amino acids (e.g., methionine and tyrosine) linked to protein damage.

Cellular Redox and Disulfide Bond Formation between Proximal Cysteines. Different microcompartments in both eukaryotic and prokaryotic cells maintain well-defined redox potentials that contribute to the maintenance of reduced cysteines necessary for optimal cell function.²⁶ Cellular redox potentials are largely determined by the ratio of reduced (GSH) to oxidized (GSSG) glutathione, which can be accurately measured using families of genetically encoded redox-sensitive fluorescent protein sensors engineered with proximal cysteine pairs whose cross-linking modulates ratiometric fluorescence sensing.²⁶ Upon fusion with the enzyme glutaredoxin (Grx) these fluorescent protein sensors provide real-time measurements of alterations in glutathione redox potentials by overcoming kinetic barriers associated with the recognition of the oxidized cysteine pair by Grx.²⁷ However, an understanding of how changes in glutathione redox potentials affect cellular responses requires complementary measurements of the status of the oxidation state between individual proximal cysteines within the cellular proteome, which is now possible using TRAP_Cy3 (Figures 4 and S5). Such measurements complement existing databases that have used *in vitro* conditions to identify proteins with redox-sensitive cysteine pairs capable of forming disulfide bonds,²⁸ and provide an ability to monitor how environmental conditions (e.g., light, oxygen, and nutrient limitation) modulate the flux through central pathways involved, for example, in the assimilation of carbon and transcriptional regulation.²⁹

Oxidative Stress and Protein Post-translational Modifications. In addition to responding to changes in overall cellular redox status (i.e., GSH/GSSH), cysteines and other amino acids (primarily methionine and tyrosine) are oxidatively modified by ROS formed in the presence of, for example, light and oxygen³⁰ (Figure S7). While oxidized cysteines (e.g., sites of S-glutathionylation or intramolecular disulfide bonds between proximal cysteines) are reduced by NADPH-dependent glutathione-reductase (GR) and thioredoxin-reductase (TrxR) enzymes,^{25a} Met(O) and NY are reduced through alternative pathways involving the action of the Trx-dependent methionine sulfoxide reductases (Msr) and a denitrase

enzyme.^{25e,31} As these post-translational protein modifications have all been shown to affect protein function, their differential reduction by specific enzyme systems offers an opportunity to fine-tune cellular metabolism in response to changing environmental conditions.^{1a–d} It is therefore of considerable interest that abundances of Met(O) and NY on cellular proteins actually decrease under environmental conditions that promote cysteine oxidation (and formation of disulfide bonds between proximal cysteines) (Figure 5). The inverse relationship between redox-active cysteine oxidation and the oxidative damage to other sensitive amino acids (i.e., methionine and tyrosine) suggests the presence of *in vivo* regulatory mechanisms that minimize widespread oxidative protein damage through shifts in metabolism as a result of post-translational oxidative modifications to proximal cysteines that function to decrease the production of ROS (Figure 6). Alternatively, there may be a coordinate up-regulation of Msr and denitrase enzyme activities that increase rates of repair for oxidized methionines and tyrosines under environmental conditions linked to increases in ROS formation (i.e., increased light and oxygen). However, the latter possibility is unlikely given the known specificity of Msr enzymes to recognize only a subset of solvent exposed oxidized methionines within highly disordered sequences; the majority of oxidized methionines are not substrates for Msr.^{25b–d,31b}

SUMMARY AND FUTURE DIRECTIONS

We have demonstrated the utility of the newly synthesized cell-permeable reagent TRAP_Cy3 to monitor the status of redox-sensitive cysteine pairs in living cells. Our current results demonstrate the sensitivity of redox-active cysteines to undergo disulfide bond formation in response to normal environmental conditions linked to oxidative stress, and suggest that these post-translational modifications act as redox sensors that modify intracellular metabolism as part of an adaptive response that minimizes the oxidation of other amino acids. Future measurements should extend these measurements to quantitatively consider time-dependent kinetic responses and associated changes in the bioenergetics of cellular metabolism.

ASSOCIATED CONTENT

Supporting Information

General methods and procedures for the synthesis of TRAP_Cy3, NMR spectra and assignments for structural characterization (Figure S1 and Table S1), fluorescent images comparing cellular permeability of TRAP_Cy3 and AsCy3_3 (Figure S2), absorbance and fluorescence emission spectra of TRAP_Cy3 (Figure S3), albumin sequence and identified TRAP_Cy3-bound peptides (Figure S4 and Table S2), SDS-PAGE gels showing differential labeling of cellular proteins by TRAP_Cy3 when cells are grown under carbon-limiting conditions (Figure S5), absorbance and fluorescence emission spectra showing enhanced cysteine reactivity in preparations enriched in thylakoid membranes (Figure S6), illustration depicting amino acid sensitivities to ROS (Figure S7), and SDS-PAGE gels showing the selective affinity enrichment of peptides labeled by TRAP_Cy3 following live cell labeling, cell lysis, alkylation of available cysteines, release of TRAP_Cy3, and affinity purification (Figure S8). This material is available free of charge via the Internet at <http://pubs.acs.org>.

■ AUTHOR INFORMATION

Corresponding Author

thomas.squier@pnl.gov

Notes

The authors declare no competing financial interest.

■ ACKNOWLEDGMENTS

We are grateful for helpful discussions and assistance with the controlled cultivation and environmental sampling of *Synechococcus* sp. PCC7002 and microbial mats from Yellowstone National Park from Donald A. Bryant, Eric A. Hill, Grigoriy E. Pinchuk, Sergey Stolyar, and David M. Ward. This research was supported by the Genomic Science Program (GSP), Office of Biological and Environmental Research (OBER), U.S. Department of Energy (DOE), and is a contribution of the PNNL Biofuels and Foundational Scientific Focus Areas (SFAs). Portions of this work were supported by a DOE early career research award (to W.J.Q.). PNNL is a multiprogram National Laboratory operated by Battelle for the DOE under Contract No. DE-AC05-76RLO 1830.

■ REFERENCES

- (1) (a) Dolwick, K. M.; Schmidt, J. V.; Carver, L. A.; Swanson, H. I.; Bradfield, C. A. *Mol. Pharmacol.* **1993**, *44*, 911. (b) Xiong, Y.; Chen, B.; Shi, L.; Fredrickson, J. K.; Bigelow, D. J.; Squier, T. C. *Biochemistry* **2011**, *50*, 9738. (c) Pfeiffer, A.; Schmidt, T.; Holler, T.; Herrmann, H.; Pehl, C.; Wendl, B.; Kaess, H. *Eur. J. Clin. Pharmacol.* **1993**, *44*, 219. (d) Poole, L. B.; Nelson, K. J. *Curr Opin Chem Biol* **2008**, *12*, 18. (e) Jacob, C.; Giles, G. I.; Giles, N. M.; Sies, H. *Angew. Chem., Int. Ed.* **2003**, *42*, 4742. (f) Walsh, C. T. *Posttranslational Modifications of Proteins: Expanding Nature's Inventory*; Roberts and Company Publishers: Greenwood Village, CO, 2006.
- (2) Drabkova, M.; Matthijs, H. C. P.; Admiraal, W.; Marsalek, B. *Photosynthetica* **2007**, *45*, 363.
- (3) (a) Silva, G. M.; Netto, L. E.; Simoes, V.; Santos, L. F.; Gozto, F. C.; Demasi, M. A.; Oliveira, C. L.; Bicev, R. N.; Klitzke, C. F.; Sogayar, M. C.; Demasi, M. *Antioxid. Redox Signal.* **2012**, *16*, 1183. (b) McStay, G. P.; Clarke, S. J.; Halestrap, A. P. *Biochem. J.* **2002**, *367*, 541. (c) Moreno, J.; Garcia-Murria, M. J.; Marin-Navarro, J. J. *Exp. Bot.* **2008**, *59*, 1605. (d) Evangelista, A. M.; Thompson, M. D.; Weisbrod, R. M.; Pimental, D. R.; Tong, X.; Bolotina, V. M.; Cohen, R. A. *Antioxid. Redox Signal.* **2012**, *17*, 1099. (e) Hill, B. G.; Bhatnagar, A. J. *Mol. Cell. Cardiol.* **2012**, *52*, 559.
- (4) (a) Leonard, S. E.; Reddie, K. G.; Carroll, K. S. *ACS Chem. Biol.* **2009**, *4*, 783. (b) Weerapana, E.; Wang, C.; Simon, G. M.; Richter, F.; Khare, S.; Dillon, M. B.; Bachovchin, D. A.; Mowen, K.; Baker, D.; Cravatt, B. F. *Nature* **2010**, *468*, 790.
- (5) Leonard, S. E.; Carroll, K. S. *Curr. Opin. Chem. Biol.* **2011**, *15*, 88.
- (6) Davis, O. B.; Bishop, A. C. *Bioconjugate Chem.* **2012**, *23*, 272.
- (7) (a) Griffin, B. A.; Adams, S. R.; Tsien, R. Y. *Science* **1998**, *281*, 269. (b) Nelson, K. J.; Klomsiri, C.; Codreanu, S. G.; Soito, L.; Liebler, D. C.; Rogers, L. C.; Daniel, L. W.; Poole, L. B. *Methods Enzymol.* **2010**, *473*, 95. (c) Seo, Y. H.; Carroll, K. S. *Angew. Chem., Int. Ed.* **2011**, *50*, 1342.
- (8) (a) Huang, C.; Yin, Q.; Zhu, W.; Yang, Y.; Wang, X.; Qian, X.; Xu, Y. *Angew. Chem., Int. Ed.* **2011**, *50*, 7551. (b) Gitler, C.; Zarmi, B.; Kalef, E. *Anal. Biochem.* **1997**, *252*, 48.
- (9) (a) Vazquez, M. E.; Blanco, J. B.; Salvadori, S.; Trapella, C.; Argazzi, R.; Bryant, S. D.; Jinsmaa, Y.; Lazarus, L. H.; Negri, L.; Giannini, E.; Lattanzi, R.; Colucci, M.; Balboni, G. *J. Med. Chem.* **2006**, *49*, 3653. (b) Nandhikonda, P.; Begaye, M. P.; Cao, Z.; Heagy, M. D. *Chem. Commun. (Camb.)* **2009**, 4941. (c) Katritsky, A. R.; Ozcan, S.; Todadze, E. *Org. Biomol. Chem.* **2010**, *8*, 1296.
- (10) Liu, M.; Durfee, T.; Cabrera, J. E.; Zhao, K.; Jin, D. J.; Blattner, F. R. *J. Biol. Chem.* **2005**, *280*, 15921.
- (11) Klatt, C. G.; Wood, J. M.; Rusch, D. B.; Bateson, M. M.; Hamamura, N.; Heidelberg, J. F.; Grossman, A. R.; Bhaya, D.; Cohan, F. M.; Kuhl, M.; Bryant, D. A.; Ward, D. M. *ISME J.* **2011**, *5*, 1262.
- (12) Melnicki, M. R.; Pinchuk, G. E.; Hill, E. A.; Kucek, L. A.; Fredrickson, J. K.; Konopka, A.; Beliaev, A. S. *mBio* **2012**, *3*, e00197.
- (13) Liu, T.; Qian, W. J.; Camp, D. G., II; Smith, R. D. *Methods Mol. Biol.* **2007**, *359*, 107.
- (14) (a) Kelly, R. T.; Page, J. S.; Luo, Q.; Moore, R. J.; Orton, D. J.; Tang, K.; Smith, R. D. *Anal. Chem.* **2006**, *78*, 7796. (b) Livesay, E. A.; Tang, K.; Taylor, B. K.; Buschbach, M. A.; Hopkins, D. F.; LaMarche, B. L.; Zhao, R.; Shen, Y.; Orton, D. J.; Moore, R. J.; Kelly, R. T.; Udseth, H. R.; Smith, R. D. *Anal. Chem.* **2008**, *80*, 294.
- (15) Ernst, L. A.; Gupta, R. K.; Mujumdar, R. B.; Waggoner, A. S. *Cytometry* **1989**, *10*, 3.
- (16) (a) Mujumdar, R. B.; Ernst, L. A.; Mujumdar, S. R.; Lewis, C. J.; Waggoner, A. S. *Bioconjugate Chem.* **1993**, *4*, 105. (b) Jung, M. E.; Kim, W. J. *Bioorg. Med. Chem.* **2006**, *14*, 92. (c) Xu, Y.; Liu, Y.; Qian, X. *J. Photochem. Photobiol., A* **2007**, *190*, 1.
- (17) Cao, H.; Xiong, Y.; Wang, T.; Chen, B.; Squier, T. C.; Mayer, M. U. *J. Am. Chem. Soc.* **2007**, *129*, 8672.
- (18) Chen, B.; Cao, H.; Yan, P.; Mayer, M. U.; Squier, T. C. *Bioconjugate Chem.* **2007**, *18*, 1259.
- (19) (a) Boschek, C. B.; Squier, T. C.; Bigelow, D. J. *Biochemistry* **2007**, *46*, 4580. (b) Chen, B.; Mayer, M. U.; Markillie, L. M.; Stenoien, D. L.; Squier, T. C. *Biochemistry* **2005**, *44*, 905.
- (20) (a) Noort, D.; Hulst, A. G.; de Jong, L. P.; Benschop, H. P. *Chem. Res. Toxicol.* **1999**, *12*, 715. (b) Turell, L.; Carballal, S.; Botti, H.; Radi, R.; Alvarez, B. *Braz. J. Med. Biol. Res.* **2009**, *42*, 305. (c) Li, H.; Grigoryan, H.; Funk, W. E.; Lu, S. S.; Rose, S.; Williams, E. R.; Rappaport, S. M. *Mol. Cell. Proteomics* **2011**, *10*, M110 004606.
- (21) (a) Su, D.; Shukla, A. K.; Chen, B.; Kim, J.-S.; Nakayasu, E.; Qu, Y.; Aryal, U.; Weitz, K.; Clauss, T. R. W.; Monroe, M. E.; Camp, D. G., II; Bigelow, D. J.; Smith, R. D.; Kulkarni, R. N.; Qian, W.-J. *Free Radic. Biol. Med.* **2013**, *57*, 68–78. (b) Liu, T.; Qian, W. J.; Strittmatter, E. F.; Camp, D. G., II; Anderson, G. A.; Thrall, B. D.; Smith, R. D. *Anal. Chem.* **2004**, *76*, 5345.
- (22) Revsbech, N. P.; Ward, D. M. *Appl. Environ. Microbiol.* **1983**, *45*, 755.
- (23) Ward, D. M.; Ferris, M. J.; Nold, S. C.; Bateson, M. M. *Microbiol. Mol. Biol. Rev.* **1998**, *62*, 1353.
- (24) (a) Feng, W. K.; Wang, L.; Lu, Y.; Wang, X. Y. *FEBS J.* **2011**, *278*, 3419. (b) Wu, G.; Ortiz-Flores, G.; Ortiz-Lopez, A.; Ort, D. R. *J. Biol. Chem.* **2007**, *282*, 36782. (c) Lima, A.; Lima, S.; Wong, J. H.; Phillips, R. S.; Buchanan, B. B.; Luan, S. *Proc. Natl. Acad. Sci. U.S.A.* **2006**, *103*, 12631. (d) Lamkemeyer, P.; Laxa, M.; Collin, V.; Li, W.; Finkemeier, I.; Schottler, M. A.; Holtkamp, V.; Tognetti, V. B.; Issakidis-Bourguet, E.; Kandlbinder, A.; Weis, E.; Miginiac-Maslow, M.; Dietz, K. J. *Plant J.* **2006**, *45*, 968.
- (25) (a) Banerjee, R. In *Redox Biochemistry*; Banerjee, R., Becker, D., Dickman, M., Gladyshev, V., Ragsdale, S., Eds.; John Wiley & Sons, Inc.: Hoboken, NJ, 2008; p 1. (b) Bigelow, D. J.; Squier, T. C. *Mol. Biosyst.* **2011**, *7*, 2101. (c) Bigelow, D. J.; Squier, T. C. *Biochim. Biophys. Acta* **2005**, *1703*, 121. (d) Chen, B.; Markillie, L. M.; Xiong, Y.; Mayer, M. U.; Squier, T. C. *Biochemistry* **2007**, *46*, 14153. (e) Smallwood, H. S.; Lourette, N. M.; Boschek, C. B.; Bigelow, D. J.; Smith, R. D.; Pasa-Tolic, L.; Squier, T. C. *Biochemistry* **2007**, *46*, 10498.
- (26) Lohman, J. R.; Remington, S. J. *Biochemistry* **2008**, *47*, 8678.
- (27) Morgan, B.; Sobotta, M. C.; Dick, T. P. *Free Radic. Biol. Med.* **2011**, *51*, 1943.
- (28) (a) Bonetto, V.; Ghezzi, P. In *Redox Proteomics: From Protein Modifications to Cellular Dysfunction and Diseases*; Dalle-Donne, I., Scaloni, A., Butterfield, D. A., Eds.; Wiley & Sons, Inc.: Hoboken, NJ, 2006. (b) Scaloni, A. In *Redox Proteomics: From Protein Modifications to Cellular Dysfunction and Diseases*; Dalle-Donne, I., Scaloni, A., Butterfield, D. A., Eds.; Wiley & Sons, Inc.: Hoboken, NJ, 2006; p 59. (c) Brown, J. R.; Hartley, B. S. *Biochem. J.* **1966**, *101*, 214. (d) Wong, J. H.; Cai, N.; Balmer, Y.; Tanaka, C. K.; Vensel, W. H.;

- Hurkman, W. J.; Buchanan, B. B. *Phytochemistry* **2004**, *65*, 1629.
- (e) Yano, H.; Kuroda, S.; Buchanan, B. B. *Proteomics* **2002**, *2*, 1090.
- (29) (a) Montrichard, F.; Alkhalifioui, F.; Yano, H.; Vensel, W. H.; Hurkman, W. J.; Buchanan, B. B. *J. Proteomics* **2009**, *72*, 452.
- (b) Lindahl, M.; Kieselbach, T. *J. Proteomics* **2009**, *72*, 416.
- (30) (a) Morris, J. J.; Johnson, Z. I.; Szul, M. J.; Keller, M.; Zinser, E. R. *Plos One* **2011**, *6*, e16805. (b) Abele-Oeschger, D.; Tug, H.; Rottgers, R. *Limnol. Oceanogr.* **1997**, *42*, 1406.
- (31) (a) Ejiri, S. I.; Weissbach, H.; Brot, N. *Anal. Biochem.* **1980**, *102*, 393. (b) Xiong, Y.; Chen, B.; Smallwood, H. S.; Urbauer, R. J.; Markille, L. M.; Galeva, N.; Williams, T. D.; Squier, T. C. *Biochemistry* **2006**, *45*, 14642.
- (32) Tsodikov, O. V.; Record, M. T., Jr.; Sergeev, Y. V. *J. Comput. Chem.* **2002**, *23*, 600.